Supplementary Information (SI) for ChemComm.
This journal is © The Royal Society of Chemistry 2026

Supplementary Information

Molecular Engineering of Excited-State Dynamics via ICT toward a Cross-Reactive Single-Fluorophore Array for Discriminative Sensing of VOCs

Nan An, Luwen Zhang, Zhiyuan Yin, Mengxuan Xing, Yifan Xue, Ruijuan Wen, Junlin Yan, Jing Liu*, Yu Fang

Key Laboratory of Applied Surface and Colloid Chemistry, Ministry of Education, School of Chemistry & Chemical Engineering, Shaanxi Normal University, Xi'an, 710062, People's Republic of China
E-mail: jliu@snnu.edu.cn

Table of Contents

1. General experimental information

1.1 Solvents and regents

All chemical reagents and solvents were purchased from commercial suppliers and used without further purification, unless otherwise noted. Products were purified by column chromatography using silica gel (300-400 mesh). The spectroscopic measurements were conducted under ambient conditions using spectroscopic grade solvents. All air-sensitive reactions were carried out under nitrogen atmosphere.

1.2 Preparation of gas-sensing samples

Ten milliliters each of *n*-pentane, *n*-hexane, *n*-heptane, chloroform, tetrahydrofuran, acetone, and acetonitrile were separately placed into dry, clean amber glass vials. The vials were sealed and allowed to equilibrate at 298 K for 24 h to establish vapor–liquid equilibrium. The headspace vapor in each vial was thereby regarded as the saturated vapor of the corresponding volatile organic compound (VOC). Test gases of varying concentrations were obtained by sampling or diluting the saturated vapor using a gas-tight glass syringe (nominal volume: 100 mL).

1.3 Preparation of the BDP1/C1 gel in toluene

A toluene stock solution of **BDP1** (500 μmol/L) was prepared. Subsequently, 0.025 g of gelator **C1**[1] was added to 1 mL of this stock solution, and the mixture was heated to 363 K to achieve complete dissolution. The resulting hot solution was then cooled and allowed to stand at 289 K, whereupon a transparent gel formed.

1.4 Fabrication of the BDP1/C1 co-assembled film and solid state BDP1 film

A co-assembled fluorescent film and a solid state **BDP1** film were prepared via drop-casting for subsequent use. Specifically, 20 μL of the **BDP1**/**C1** precursor toluene solution and 20 μL of a **BDP1** toluene stock solution were uniformly deposited onto separate clean glass substrates. After drying at 323 K for 12 h, the corresponding films were obtained.

2. Characterization techniques

2.1 Nuclear magnetic resonance (NMR) spectroscopy

^{1}H NMR and ^{13}C NMR spectra were recorded on a Bruker AV 600 spectrometer (^{1}H: 600 MHz, ^{13}C: 151 MHz) at 298 K. Chemical shifts (δ, in ppm) are referenced to tetramethylsilane (TMS, δ = 0.00 ppm). 2D ^{1}H-^{1}H NOESY spectra were measured on JEOL 400 spectrometer (^{1}H: 400 MHz, ^{13}C: 101 MHz). For temperature-dependent measurements, the sample was stabilized at the corresponding temperature for 10 min.

2.2 Mass spectrometry

High-resolution electrospray ionization mass spectrometry (HR-ESI-MS) was obtained on a Bruker maXis impact Q-TOF mass spectrometer equipped with an Ultimate 3000 HPLC system.

2.3 Fourier-transform infrared spectroscopy

Fourier-transform infrared (FT-IR) spectra were acquired on a Bruker Vertex 70 spectrometer. Samples were prepared as pellets using spectroscopic-grade potassium bromide (KBr) and measured in transmission mode.

2.4 UV-vis absorption spectroscopy

UV-vis absorption spectra in solution were recorded on a Hitachi U-3900/3900H spectrophotometer at room temperature, extinction coefficients were calculated from Lambert-Beer's law, $A=\varepsilon bc$, where A is the absorbance, ε is the extinction coefficients, b is the length of the cell, and c represents the concentration of the compound under study.

2.5 Steady-state fluorescence spectroscopy

Fluorescence emission spectra and lifetime data were acquired on an Edinburgh FLS980 spectrofluorometer equipped with time-correlated single-photon counting (TCSPC) capability. Measurements were carried out using a 1 cm path length four-window quartz cuvette. A 450 W xenon lamp served as the excitation source for steady-state spectra, while a 510 nm laser was used for lifetime measurements.

2.6 Photoluminescence quantum yield

The absolute photoluminescence quantum yield (Φ) was measured on a Hamamatsu C9920-02G system, comprising the C9920-02G system and its dedicated PMA-12 software for data acquisition and analysis.

2.7 Cyclic voltammograms

Cyclic voltammograms (CVs) tests were performed using a CH instruments (model CHI 660E Electrochemical Analyzer). The solution was bubbled with argon for 30 min before analysis. CVs were obtained in dry dichloromethane containing 0.1 M $Bu_4N(PF_6)$ as the supporting electrolyte with a three-compartment cell using a 0.07 cm^2 glassy carbon (GC) electrode as the working electrode,

Ag/Ag^+ as the reference electrode, and platinum wire as the counter electrode. The GC electrode was polished with α-Al_2O_3 (50 nm) and washed with distilled H_2O and absolute ethanol. Ferrocene was added at the end of the measurement as an internal standard.

2.8 Femtosecond transient absorption spectroscopy

The femtosecond transient absorption (fs-TA) setup used for this study was based on a PHAROS laser system from Light Conversion (1030 nm, < 190 fs, 200 μJ/pulse, and 100 kHz repetition rate), nonlinear frequency mixing techniques and the Femto-TA100 spectrometer (Time-Tech Spectra). Briefly, the 1030 nm output pulse from the regenerative amplifier was split in two parts with an 80% beam splitter. The reflected part was used to pump an ORPHEUS Optical Parametric Amplifier (OPA) which generates a wavelength-tunable laser pulse from 300 nm to 15 μm. Here, 540 nm laser were used as pump beam. The transmitted 1030 nm beam was split again into two parts. One part with less than 50% was attenuated with a neutral density filter and focused into a YAG window to generate a white light continuum from 500 nm to 1600 nm used for probe beam. The probe beam was focused with an Ag parabolic reflector onto the sample. After the sample, the probe beam was collimated and then focused into a fiber-coupled spectrometer with CMOS sensors and detected at a frequency of 10 kHz. The intensity of the pump pulse used in the experiment was controlled by a variable neutral-density filter wheel. The delay between the pump and probe pulses was controlled by a motorized delay stage. The pump pulses were chopped by a synchronized chopper at 5 kHz and the absorbance change was calculated with two adjacent probe pulses (pump-blocked and pump-unblocked). During the transient measurements, the sample solution was stirred. All experiments were performed at 23 ± 2 °C.

3. Sensing performance comparison: BDP1/C1 sensor versus reported fluorescent sensors

Table S1 Performance comparison of single fluorophore-based sensors for the detection of VOCs vapor

Fluorophores	Sensing analytes	Discrimination among analytes	Response time	Recovery time	LOD/ppm	Reusability	Publication	Ref.
BODIPY derivative	***n*-pentane, *n*-hexane, *n*-heptane, $CHCl_3$, THF, acetone, CH_3CN**	**Yes**	***n*-pentane/3.3 s $CHCl_3$/8.1 s**	***n*-pentane/27.6 s $CHCl_3$/19.9 s**	***n*-pentane/758 $CHCl_3$/259**	**80 cycles**	**This work**	
Naphthylamine/ carborane derivative	toluene, THF, CH_3CN, Pr_2NH, Et_2S	--	toluene/59 s, Et_2S/16 s, Pr_2NH/60 s	toluene/8 s, Et_2S/15 s, Pr_2NH/11 s	toluene/55.5 Et_2S/54.9, Pr_2NH/43	11 cycles	Anal. Chem. **2026**, 98, 4687-4695	18
Boron-oxygen group/carborane derivative	benzene, toluene, ethylbenzene, *o*-xylene, *m*-xylene, *p*-xylene	--	4 s	< 80 s	30.9, 44.8, 34.7, 44.6, 30.9, 69.4	30 cycles	Sens. Actuators B Chem. **2025**, 441, 137986	19
Triazacoronene derivatives	nitrobenzene	--	120 s	--	--	--	ACS Sens. **2024**, 9, 251-261	20
Dibenzothiophene/ carborane derivative	THF benzene	--	6 s 9 s	3 s 20 s	15600 24729	10 cycles	Anal. Chem. **2023**, 95, 6637-6645	21
Perylene-monoamide/ carborane derivative	acetone	--	1 s	< 10 s	2.2×10^{-6}	100 cycles	CCS Chem. **2023**, 5, 2922-2932	22
Perylene bisimide/ carborane derivative	*n*-pentane, *n*-hexane, *n*-heptane, *n*-octane	--	*n*-pentane < 5 s	*n*-pentane < 5 s	*n*-pentane/10	90 cycles	Angew. Chem. Int. Ed. **2022**, 61, e202207619	1
Perylene bisimide/metallacycle complex	*n*-pentane, *n*-hexane, *n*-heptane, *n*-octane, *n*-nonane, *n*-decane	--	*n*-hexane/1.7 s	*n*-hexane/2.7 s	*n*-pentane/13.22 *n*-hexane/1.99 *n*-decane/0.24	100 cycles	Anal. Chem. **2021**, 93, 16051-16058	23
Au(III) complex/ carborane	acetone, 2-pentanone, 3-pentanone, cyclopentanone, cyclohexanone, 2-heptanone, 4-heptanone, cycloheptanone	--	cyclohexanone /6.5 s acetone/4.5 s	< 60 s	cyclohexanone /0.08 acetone/13.0	50 cycles	ACS Appl. Mater. Interfaces **2021**, 13, 5625-5633	24

4. Synthesis and characterization

4.1 Synthesis routes

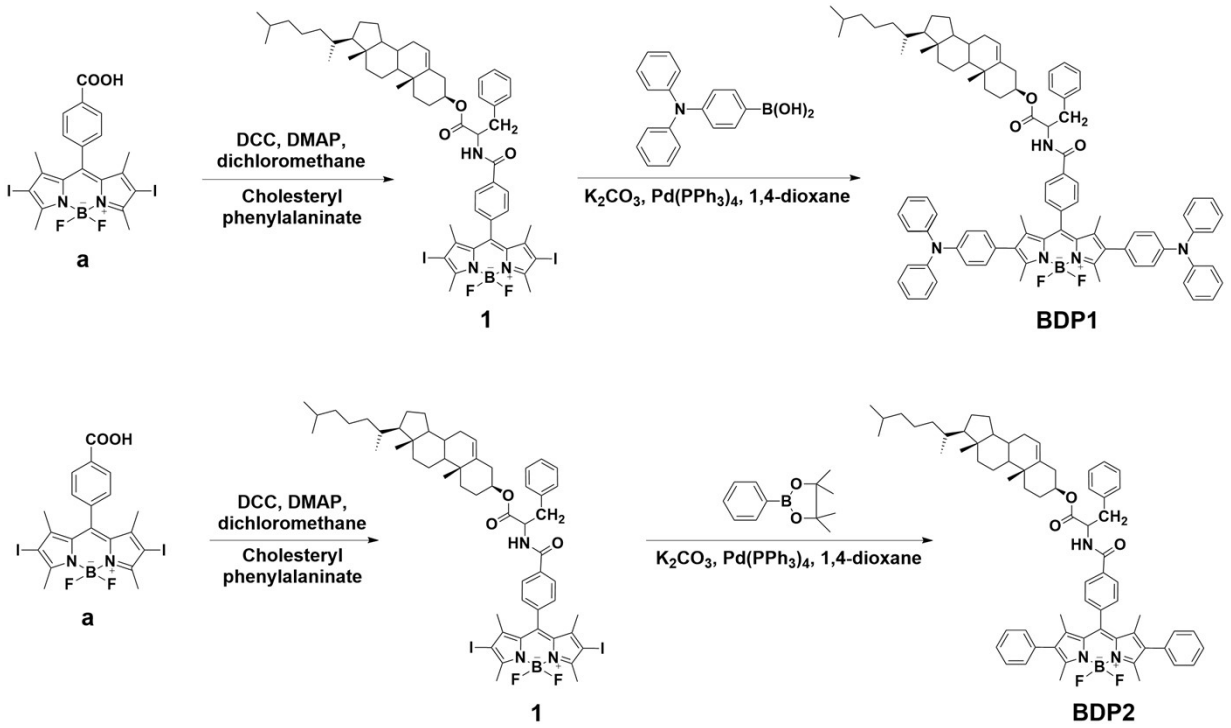

Scheme S1 Synthetic routes of **BDP1** and **BDP2**.

4.2 Synthesis of compound 1

Compound a[2] (453 mg, 0.73 mmol) and N, N'-Dicyclohexylcarbodiimide (DCC, 151 mg, 0.73 mmol), 4-Dimethylaminopyridine (DMAP, 9 mg, 73 mmol) were dissolved in dichloromethane (80 mL). After the solution was stirred for 30 min at 0 ℃, cholesteryl phenylalanine[3] (779 mg, 1.46 mmol) was added to the solution, then the mixture was stirred at room temperature for 20 h. The reaction mixture was filtered, and filtrate washed with 0.01 mol/L HCl (100 mL×3), 0.01 mol/L aqueous solution of NaOH (100 mL×3) and water (100 mL×3). The organic layers were dried over anhydrous Na_2SO_4, and concentrated under reduced pressure. The crude product was purified by

column chromatography (silica gel, eluent: dichloromethane/petroleum ether = 5:1, *v*/*v*) to give compound 1 as a red solid (yield: 50%). FTIR (KBr, ν_{max}/cm^{-1}): 3438 (N-H), 2947 (-C-H), 1743 (C=O), 1654 (C=N), 1531 (C=C), 1170 (C-O). ^{1}H NMR δ_H (600 MHz, $CDCl_3$, Me_4Si): 7.85 (d, J = 8.2 Hz, 2H, phenyl ring), 7.29 (d, J = 8.2 Hz, 2H, phenyl ring), 7.23-7.31 (m, 5H, benzyl), 6.32 (d, J = 7.5 Hz, 1H, NH), 5.34 (s, 1H, alkenyl), 4.99-5.03 (m, 1H, HC-NH), 4.59-4.63 (m, 1H, CH_2), 3.21-3.24 (m, 2H, CH_2 (C_6H_5)), 2.58 (s, 6H, CCH_3), 1.29 (s, 6H, CCH_3), 0.62-2.31 (m, 43H, cholesteryl protons). ^{13}C NMR δ_C (600 MHz, $CDCl_3$, Me_4Si): 171.07 (1C, carboxyl), 167.67 (1C, amide), 165.68 (1C, benzene), 157.33 (2C, pyrrole ring), 145.09 (2C, pyrrole ring), 139.79 (1C, ethylene), 139.31 (1C, benzene), 138.33 (1C, benzene-HC-NH), 135.82 (1C, ethylene), 132.37 (2C, pyrrole ring), 130.88 (2C, benzene), 129.49 (2C, benzene), 128.84 (2C, benzene), 128.45 (2C, benzene), 128.13 (1C, benzene), 127.27 (1C, ethylene), 123.13 (1C, pyrrole ring), 75.90 (1C, cyclohexane), 65.54 (1C, pyrrole ring), 56.71 (1C, cyclopentane), 56.18 (1C, cyclopentane), 53.82 (1C, C-NHCO), 50.06 (1C, cyclohexane), 42.34 (1C, cyclopentane), 39.73 (1C, CH_2 (C_6H_5)), 30.59 (1C, cyclohexane), 19.19 (1C, alkyl chain), 13.72 (2C, pyrrole ring -CH_3), 19.19 (2C, pyrrole ring -CH_3). MS (*m*/*z*, APCI$^+$): calculated for $C_{56}H_{70}BF_2I_2N_3O_3$, 1136.3646 ([M+H]$^+$), found: 1136.3637. Elemental analysis (%): calculated for $C_{56}H_{70}BF_2I_2N_3O_3$: C 59.22, H 6.21, N 3.70, found: C 59.68, H 6.29, N 3.62.

4.3 Synthesis of BDP1

Compound 1 (341 mg, 0.30 mmol) and [4-(diphenyl amino) phenyl] boronic acid (347 mg, 1.20 mmol) were dissolved in dry 1, 4-dioxane (50 mL). The solution was degassed by bubbling with N_2 for 30 min. Then, $Pd(PPh_3)_4$ (87 mg, 0.075 mmol) and an aqueous solution of K_2CO_3 (2 mol/L, 2 mL) were added, and the resulting mixture was stirred at 100 °C for 24 h. The organic solvent was removed

under reduced pressure. The residue was successively dissolved in CH_2Cl_2 (50 mL) and washed with water (80 mL × 3). The organic layer was then dried over anhydrous Na_2SO_4 and concentrated under reduced pressure. Purification of the crude product by column chromatography (silica gel, ethyl acetate/petroleum ether = 1:7, *v*/*v*) afforded **BDP1** as a purple solid (yield: 33%). FTIR (KBr, ν_{max}/cm^{-1}): 3427 (N-H), 2937 (-C-H), 1741 (C=O), 1675 (C=N), 1596 (C=C), 1184 (C-O), 1280 (C-N). ^{1}H NMR δ_H (600 MHz, $CDCl_3$, Me_4Si): 7.92 (d, J = 8.2 Hz, 2H, phenyl ring), 7.52 (d, J = 8.2 Hz, 2H, phenyl ring), 7.06-7.35 (m, 33H, benzyl, triphenylamine), 6.72 (d, J = 7.5 Hz, 1H, NH), 5.44 (s, 1H, alkenyl), 5.02-5.05 (m, 1H, HC-NH), 4.64-4.70 (m, 1H, CH_2), 3.25-3.33 (m, 2H, CH_2 (C_6H_5)), 2.57 (s, 6H, CCH_3), 1.24 (s, 6H, CCH_3), 0.73-2.41 (m, 43H, cholesteryl protons). ^{13}C NMR δ_C (600 MHz, $CDCl_3$, Me_4Si): 171.07 (1C, carboxyl), 165.97 (1C, amide), 154.91 (1C, benzene), 147.65 (2C, benzene C-N), 146.87 (2C, pyrrole ring), 140.14 (2C, pyrrole ring), 139.35 (4C, benzene C-N), 138.66 (1C, ethylene), 135.88 (1C, benzene), 134.55 (1C, benzene-HC-NH), 133.72 (1C, ethylene), 130.84 (2C, pyrrole ring), 129.52 (8C, benzene), 129.32 (2C, benzene), 128.80 (2C, benzene), 128.59 (4C, benzene), 127.91 (1C, benzene), 127.24 (1C, ethylene), 127.09 (8C, benzene), 124.63 (2C, benzene C-pyrrole ring), 123.09 (4C, benzene), 122.97 (1C, ethylene), 75.87 (1C, cyclohexane), 56.73 (1C, cyclopentane), 56.20 (1C, cyclopentane), 53.81 (1C, C-NHCO), 50.08 (1C, cyclohexane), 42.37 (1C, cyclopentane), 39.55 (1C, CH_2 (C_6H_5)), 28.03 (1C, cyclohexane), 11.90 (1C, alkyl chain). MS (*m*/*z*, APCI$^+$): calculated for $C_{92}H_{98}BF_2N_5O_3$, 1370.7809 ([M+H]$^+$), found: 1370.7820. Elemental analysis (%): calculated for $C_{92}H_{98}BF_2N_5O_3$: C 80.62, H 7.21, N 5.11, found: C 80.70, H 7.26, N 5.11.

4.4 Synthesis of BDP2

Compound 1 (341 mg, 0.30 mmol) and 4,4,5,5-tetramethyl-2-phenyl-1,3,2-dioxaborolane (245 mg, 1.20 mmol) were dissolved in dry 1, 4-dioxane (50 mL). The solution was degassed by bubbling with N_2 for 30 min. Then, Tetrakis(triphenylphosphine)palladium ($Pd(PPh_3)_4$, 87 mg, 0.075 mmol) and an aqueous solution of K_2CO_3 (2 mol/L, 2 mL) were added, and the resulting mixture was stirred at 100 °C for 24 h. The organic solvent was removed under reduced pressure. The residue was dissolved in CH_2Cl_2 (50 mL) and washed with water (80 mL×3). The organic layers were dried over anhydrous Na_2SO_4, and concentrated under reduced pressure. The crude product was purified by column chromatography (silica gel, eluent: dichloromethane /petroleum ether = 3:1, *v*/*v*) to give **BDP2** as an orange solid (yield: 56%). ^{1}H NMR δ_H (600 MHz, $CDCl_3$, Me_4Si): 7.88 (d, J = 8.2 Hz, 2H, phenyl ring), 7.47 (d, J = 8.2 Hz, 2H, phenyl ring), 7.15-7.41 (m, 15H, phenyl ring), 6.67 (d, J = 7.5 Hz, 1H, NH), 5.39 (d, J = 4.9 Hz, 1H, alkenyl), 5.04-5.06 (m, 1H, HC-NH), 4.63-4.69 (m, 1H, CH_2), 3.26-3.27 (m, 2H, CH_2 (C_6H_5)), 2.54 (s, 6H, CCH_3), 1.29 (s, 6H, CCH_3), 0.68-2.33 (m, 43H, cholesteryl protons). ^{13}C NMR δ_C (600 MHz, $CDCl_3$, Me_4Si): 171.07 (1C, carboxyl), 167.70 (1C, amide), 154.79 (1C, benzene), 140.14 (2C, pyrrole ring), 139.31 (2C, pyrrole ring), 139.13 (2C, pyrrole ring), 138.91 (1C, ethylene), 135.84 (1C, benzene), 134.59 (1C, benzene-HC-NH), 132.36 (2C, pyrrole ring), 132.08 (2C, benzene), 130.90 (2C, benzene), 130.14 (2C, benzene), 129.49 (2C, benzene), 128.85 (4C, benzene), 128.55 (2C, benzene), 128.37 (4C, benzene), 127.94 (2C, benzene), 127.19 (1C, benzene), 123.10 (1C, ethylene), 75.83 (1C, cyclohexane), 50.03-56.70 (14C, cyclopentane), 42.37 (2C, cyclopentane), 39.55 (1C, CH_2 (C_6H_5)), 19.19-38.04 (10C, alkyl chain), 11.87-13.73 (4C, alkyl chain). MS (*m*/*z*, APCI$^+$): calculated for $C_{68}H_{80}BF_2N_3O_3$, 1036.6339 ([M+H]$^+$), found: 1036.6346. Elemental analysis (%): calculated for $C_{68}H_{80}BF_2N_3O_3$: C 78.82, H 7.78, N 4.06, found: C 77.68, H

7.80, N 4.09.

HRMS, and NMR spectra of BDP1 and BDP2:

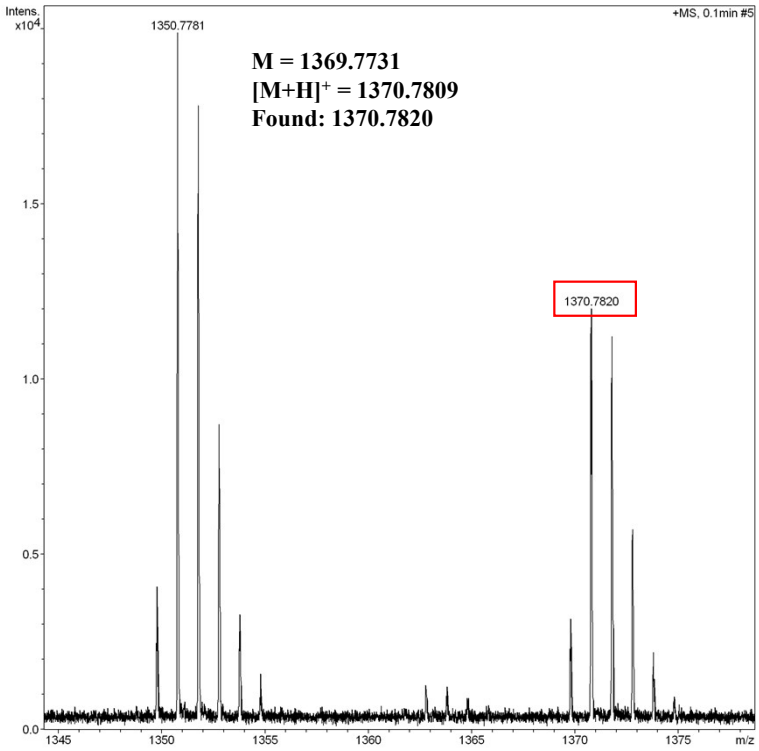

Fig. S1 The ESI-MS spectrum of **BDP1**.

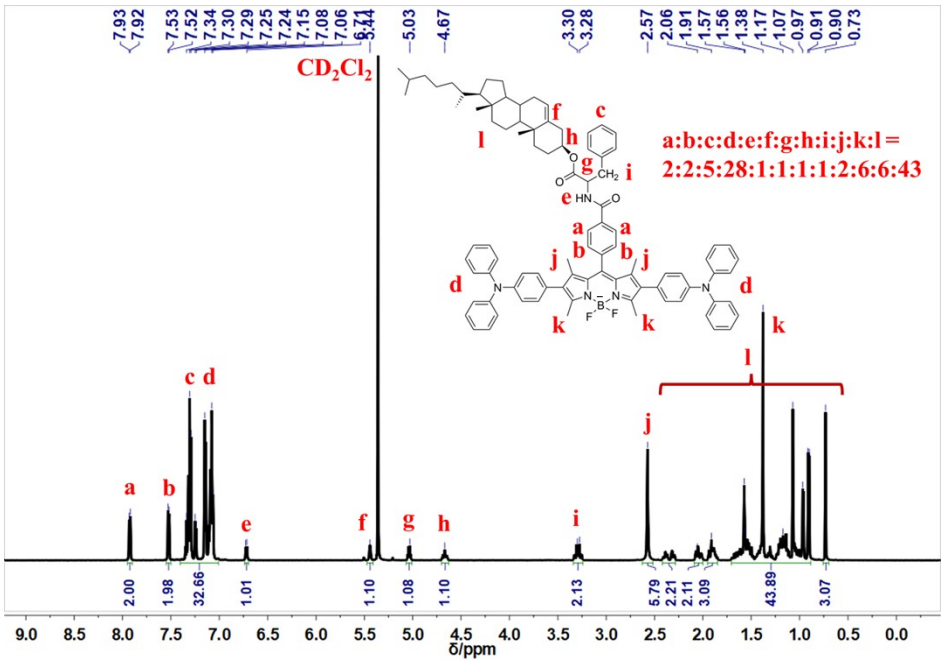

Fig. S2 The ^{1}H NMR spectrum of **BDP1** (600 MHz, $CDCl_2$-*d*, 298 K).

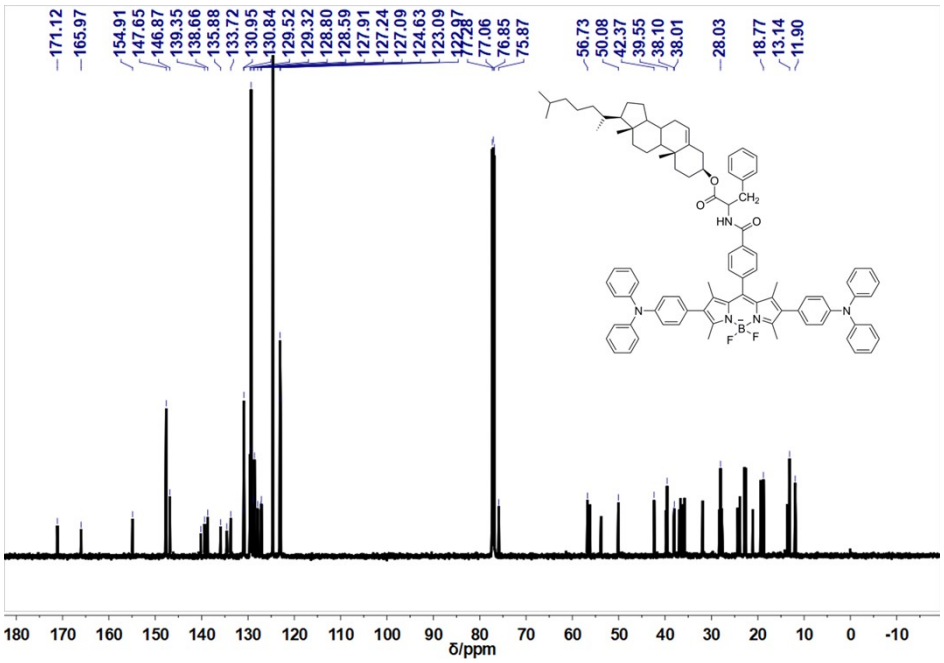

Fig. S3 The ^{13}C NMR spectrum of **BDP1** (600 MHz, $CDCl_2$-*d*, 298 K).

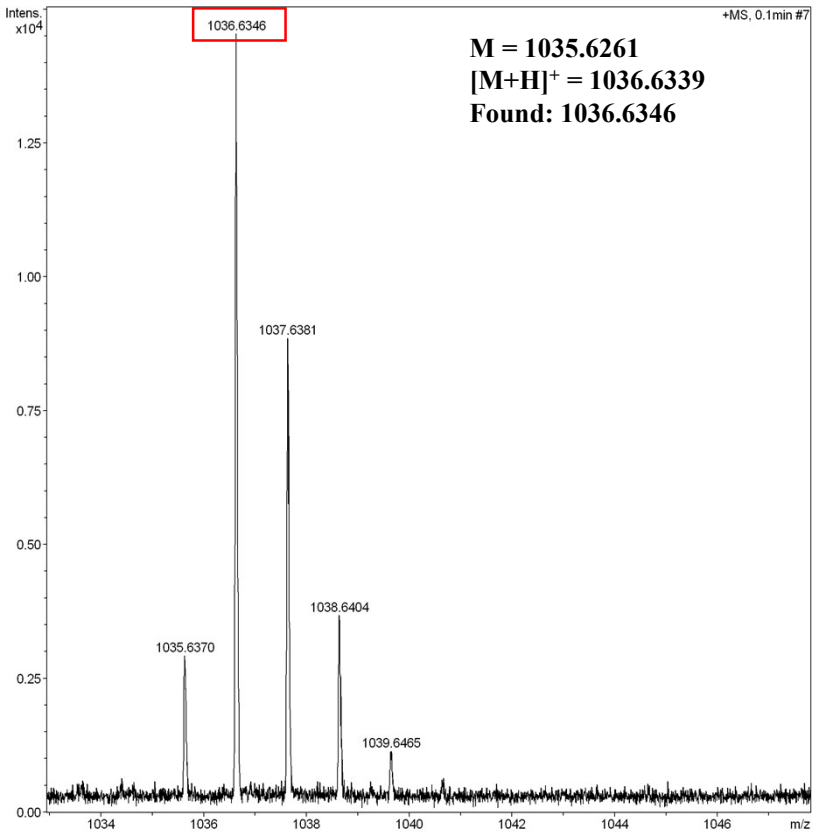

Fig. S4 The ESI-MS spectrum of **BDP2**.

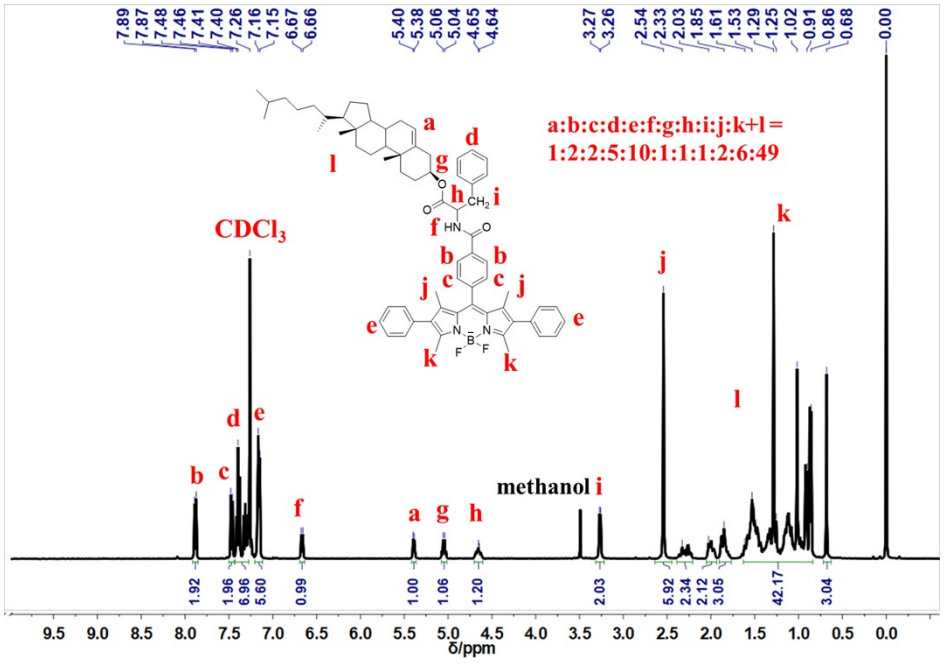

Fig. S5 The ^{1}H NMR spectrum of **BDP2** (600 MHz, $CDCl_3$-*d*, 298 K).

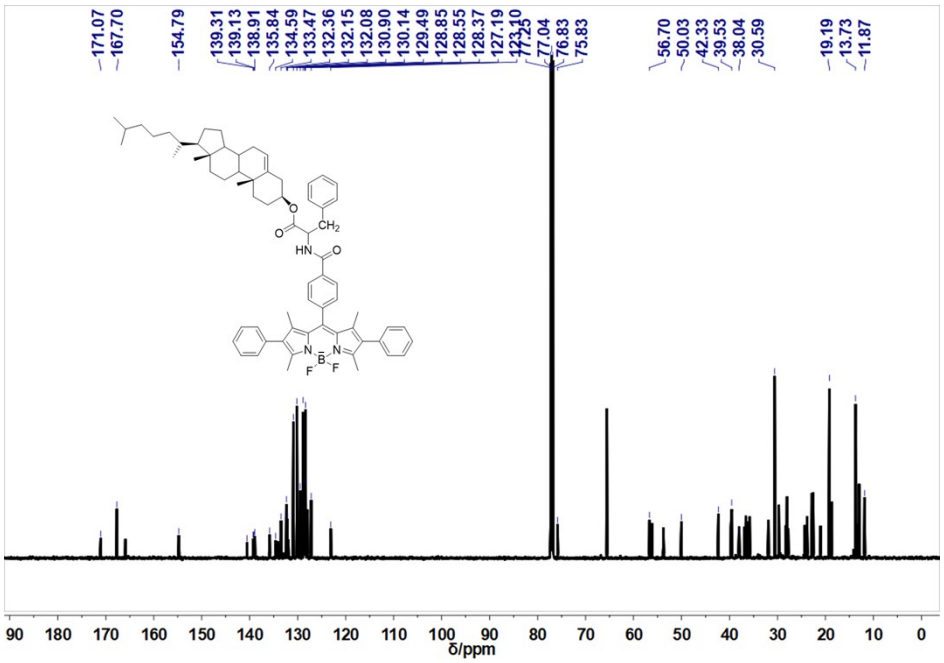

Fig. S6 The ^{13}C NMR spectrum of **BDP2** (600 MHz, $CDCl_3$-*d*, 298 K).

5. Cyclic voltammograms of BDP1 and BDP2

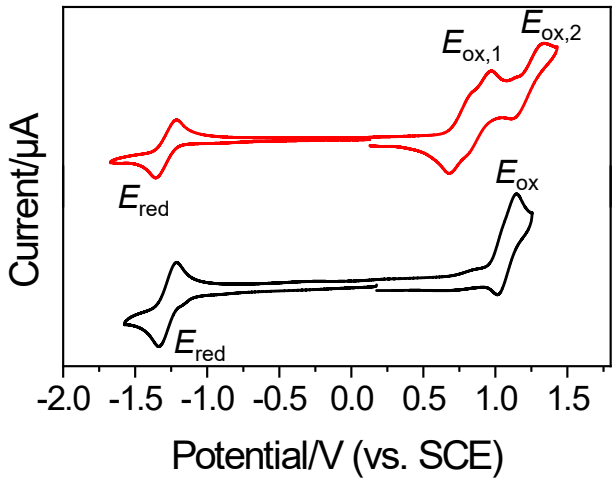

Fig. S7 Cyclic voltammograms of **BDP1** (red curve) and **BDP2** (black curve) recorded at a scan rate of 100 mV s^{-1} in 1.0 × 10^{-3} mol/L solutions under an Ar atmosphere.

Table S2. Electrochemical properties of **BDP1** and **BDP2**

Compound	E_{red}[a] (V)	$E_{ox,1}$[b] (V)	$E_{ox,2}$[b] (V)
BDP1	-1.29	0.97	1.31
BDP2	-1.27	E_{ox} = 1.14	/

a, Reduction peak potentials ($E_{red} = E_{1/2}$); *b*, Oxidation peak potentials (E_{ox}, E_{ox1}, E_{ox2}). The oxidation and reduction potentials of **BDP1** and **BDP2** were recorded versus SCE.

6. Photophysical properties of BDP1 and BDP2

Table S3. Photophysical parameters of **BDP1** and **BDP2** in various solvents

Compound Solvents	Δf	ε ($M^{-1}cm^{-1}$)	λ_{abs} (nm)	λ_{em} (nm)	$\Delta\lambda$ (nm)	Φ (%)	τ^a (ns)
BDP1							
n-hexane	0	56320	544	622	78	54.4	4.03
toluene	0.01	62960	551	648	97	32.6	2.95
1,4-dioxane	0.02	41880	547	654	107	20.2	2.30
chloroform	0.15	42760	549	684	135	11.7	1.72
ethyl acetate	0.20	72000	542	685	143	6.6	1.21
THF	0.21	55910	546	691	145	6.8	1.11
acetone	0.28	50480	543	719	222	1.1	0.52
BDP2							
n-hexane	0	86100	529	559	30	71.5	4.79
toluene	0.01	79900	532	566	34	79.9	4.62
1,4-dioxane	0.02	85700	530	562	32	78.5	5.38
chloroform	0.15	62370	532	565	33	80.1	5.05
ethyl acetate	0.20	80700	526	558	32	80.8	5.36
THF	0.21	73490	529	562	33	78.8	4.98
acetone	0.28	54370	527	559	32	76.7	5.18

a, detected at the peak wavelength of CT emission. Δf, the Lippert-Mataga polarity parameter,[4] calculated by the following equation, $\Delta f = (\varepsilon-1)/(2\varepsilon+1) - (n^2-1)/(2n^2+1)$, where ε and n are the dielectric constant and the refractive index of the solvent.

7. Solvatochromic properties of BDP1

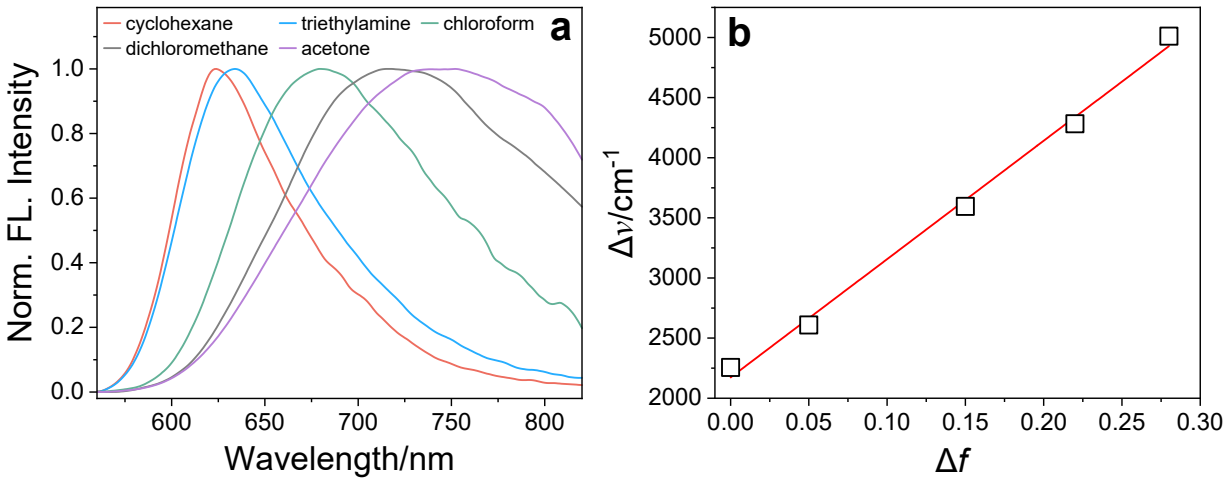

Fig. S8 (a) Fluorescence emission spectra of **BDP1** in different solvents. (b) Linear correlation between the stokes shift of **BDP1** and solvent polarity (R^2 = 0.99).

Table S4 Spectral properties of **BDP1**

Solvents	Δf	λ_{abs} (nm)	λ_{em} (nm)	$\Delta\lambda$ (nm)	$\Delta\nu$ (cm^{-1})
cyclohexane	0	548	623	75	2256
triethylamine	0.05	544	633	89	2609
chloroform	0.15	549	684	135	3595
dichloroethane	0.22	549	717	170	4282
acetone	0.28	543	765	222	5011

The Stokes shift ($\Delta\nu$) of **BDP1** was plotted against the Δf values of the corresponding solvents: cyclohexane (2256 cm^{-1}), triethylamine (2609 cm^{-1}), chloroform (3595 cm^{-1}), dichloroethane (4282 cm^{-1}), and acetone (5011 cm^{-1}) (Fig. S8 and Table S3). A strong linear correlation was observed between the Stokes shift of **BDP1** and solvent polarizability (R^2 = 0.99, Fig. S8b), indicating a clear solvatochromic effect. Using the Lippert–Mataga equation[4] (Equation S1), the difference between the excited-state and ground-state dipole moments ($\Delta\mu$) was determined to be 14.54 D from the slope of the linear fit. The ground-state dipole moment (μ_g) was calculated as 4.91 D via Density Functional Theory (DFT). Consequently, the excited-state dipole moment (μ_e) was estimated to be 19.45 D. This

large excited-state dipole moment is attributed to the charge transfer process occurring in **BDP1** upon excitation.

$$\Delta\nu = \nu_{abs} - \nu_{em} = \frac{2}{hc}\frac{(\mu_e - \mu_g)^2}{a^3} \cdot \Delta f + \text{constant} \qquad \text{(S1)}$$

Where $\Delta\nu$ represents the Stokes shift (in cm^{-1}), while ν_a and ν_{em} denote the wavenumbers (cm^{-1}) corresponding to the absorption and fluorescence emission maxima, respectively. The constant h is Planck's constant, c is the speed of light (cm/s), and a is the radius of the solvent cavity (in cm) in which the fluorophore is embedded. The value of a was estimated as 60% of the maximum calculated diameter of the optimized molecular structures, obtained from DFT simulations using the Gaussian 16 program package[5] in *n*-hexane at the CAM-B3LYP/6-31G(d,p) level of theory.[6] The parameters μ_e and μ_g refer to the dipole moments in the excited state and ground state, respectively.

8. DFT and Time-Dependent-DFT (TD-DFT) calculations

All DFT calculations were performed using the Gaussian 16 program package.[5] Geometry optimizations for both the ground state and excited states were conducted with the cam-b3lyp functional and the 6-31g(d,p) basis set.[6] The polarizable continuum model (PCM)[7] employing the linear-response (LR) formalism[8] was adopted to account for solvent effects implicitly.

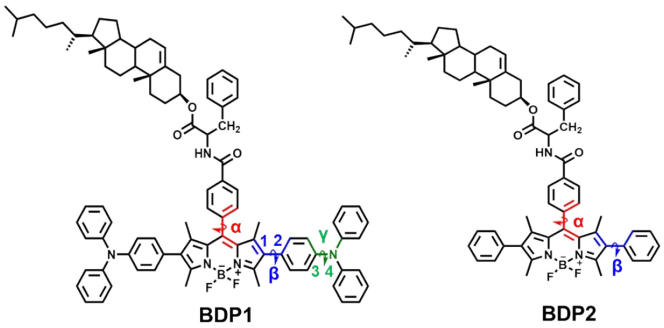

Table S5. Optimized geometry parameters (bond lengths in Å and dihedral angles in °) in S_0 and S_1-min of **BDP1** and **BDP2**, calculated at camb3lyp/6-31g(d,p) level in *n*-hexane.

Structure		d_{C1-C2}/Å	d_{C3-N4}/Å	α/°	β/°	γ/°
BDP1	S_0	1.475	1.414	79.3	127.5	39.3
	S_1-min	1.458	1.407	68.9	141.2	35.9
BDP2	S_0	1.479	/	81.6	125.9	/
	S_1-min	1.468	/	70.8	133.4	/

Table S6. The calculate molecule orbitals contribution for the S_1 state of **BDP1** and **BDP2** under the level of camb3lyp/6-31g(d,p).

Compound	Orbital	Coeff.	Contri.
1	HOMO-2 → LUMO	-0.32844	21.6%
	HOMO → LUMO	0.60798	73.9%
2	HOMO → LUMO	0.69194	95.8%

9. Transient absorption spectra of BDP1 and BDP2

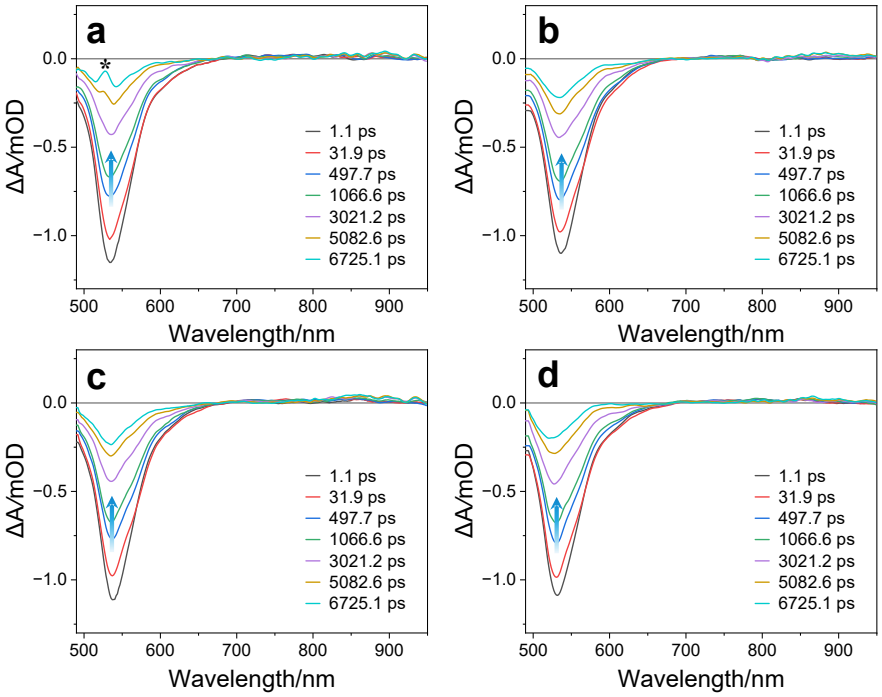

Fig. S9 fs-TA spectra of **BDP2** in (a) *n*-hexane, (b) 1,4-dioxane, (c) chloroform, and (d) ethyl acetate with a concentration of 50 μmol/L. The signal marked with an asterisk (*) originates from the laser light.

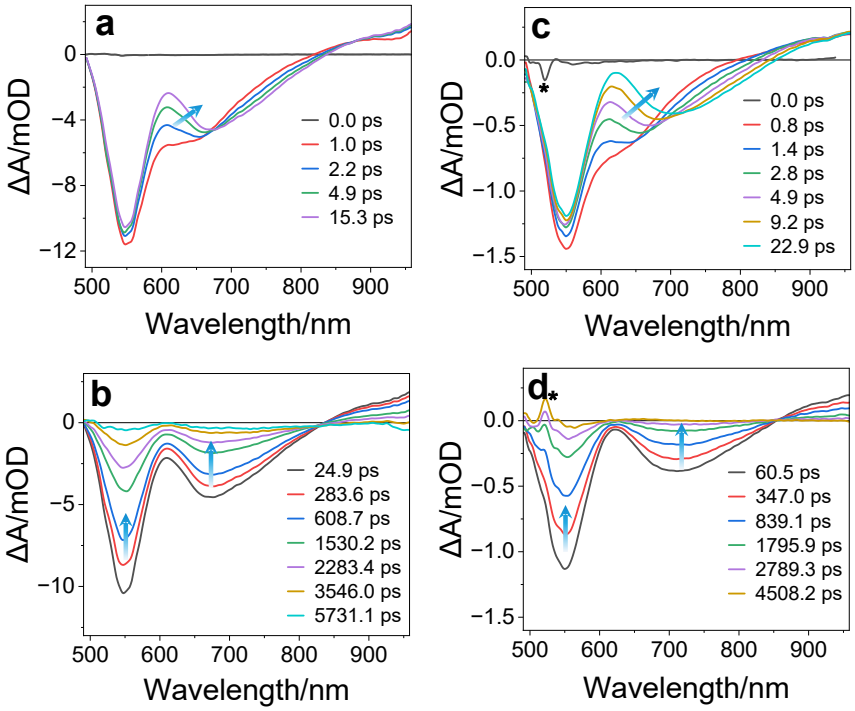

Fig. S10 fs-TA spectra of **BDP1** in (a,b) 1,4-dioxane and (c,d) chloroform. λ_{ex} = 540 nm. The signal marked with an asterisk (*) originates from the laser light.

10. Custom-built sensing platform for gas-phase sensing studies of BDP1/C1 film

All measurements were performed on a custom-built sensing platform designed for continuous monitoring of the films' fluorescence intensity. The platform integrated a circuit control board, an exhaust gas treatment unit, a sensor module, and a gas pump. All analytes under investigation were originally in the liquid state, and their vapors were sampled for analysis.

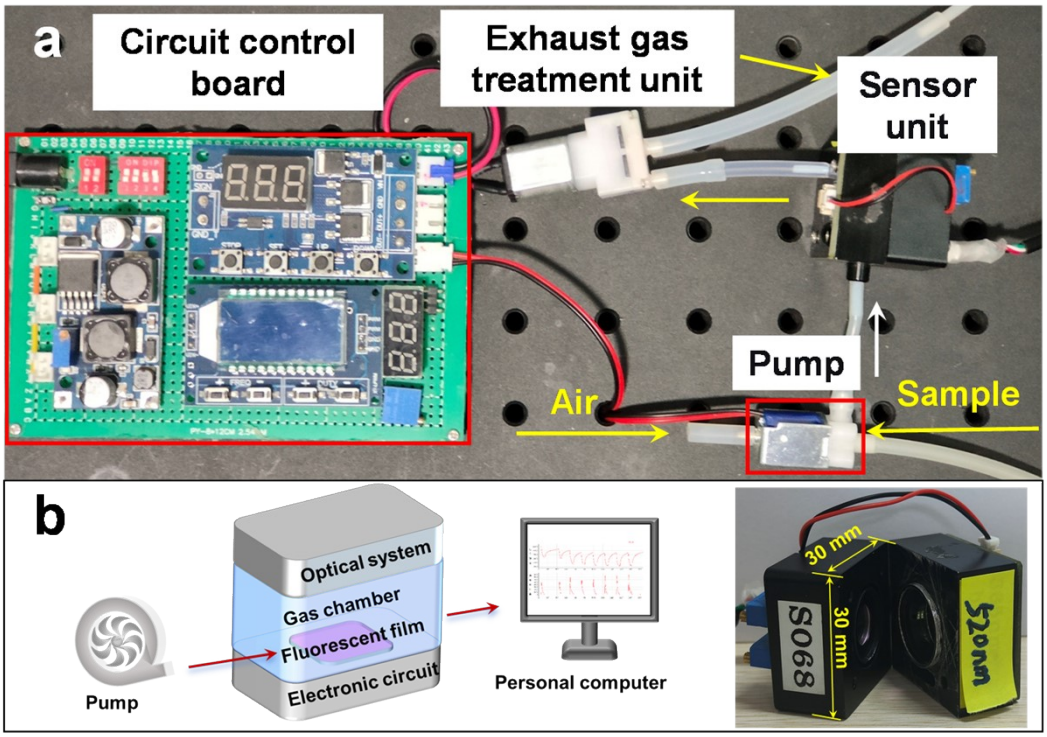

Fig. S11 (a) Photograph of the custom-built sensing platform. (b) Schematic of the internal structure and a photograph of the sensor.

11. ^{1}H-^{1}H NOESY NMR spectra of BDP1, C1 and BDP1/C1

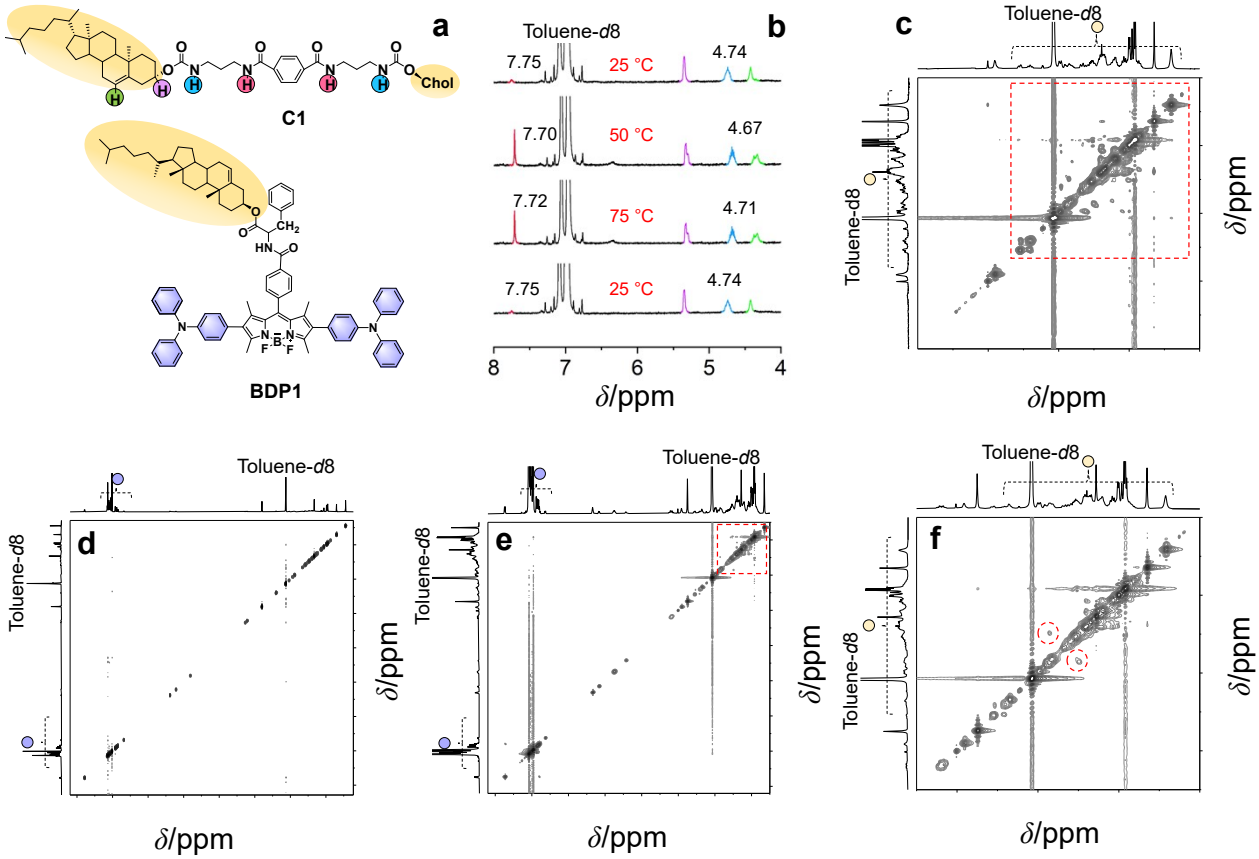

Fig. S12 (a) Chemical structures of **C1** and **BDP1** with key moieties highlighted in different colors. (b) Temperature-dependent ^{1}H NMR spectra of the **C1** gel in *d*8-toluene. (c) ^{1}H-^{1}H NOESY NMR spectrum of the **C1** gel in *d*8-toluene. (d) ^{1}H-^{1}H NOESY NMR spectrum of **BDP1** in *d*8-toluene (Concentration: 2 mg in 0.5 mL). (e) ^{1}H-^{1}H NOESY NMR spectrum of the **BDP1**/**C1** co-assembled gel in *d*8-toluene (Concentration: **BDP1**, 2 mg in 0.5 mL, **C1**, 2 mg in 0.5 mL). (f) Expanded view of the low-field region (red square in e).

12. Sensing performance of BDP1/C1 fluorescent film

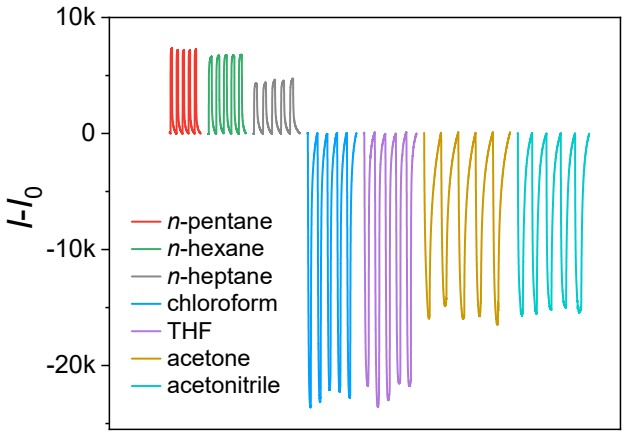

Fig. S13 Fluorescence response of **BDP1**/**C1** film to various VOCs.

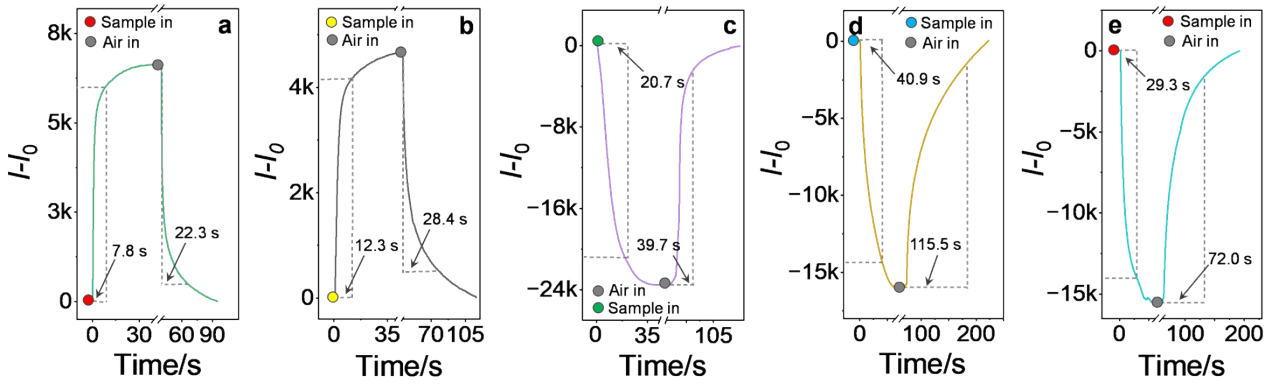

Fig. S14 Response-recovery profiles illustrating the dynamic fluorescence response of the **BDP1**/**C1** film to (a) *n*-hexane, (b) *n*-heptane, (c) tetrahydrofuran (THF), (d) acetone, and (e) acetonitrile vapors.

13. Limit of detection determination

The insets in Fig. 4e and 4f depict the calibration curves for *n*-pentane and chloroform vapors, respectively. As shown in Fig. 4e, the response intensity of the sensor exhibits a linear relationship with *n*-pentane concentration over the range of 3180–15900 ppm, yielding a correlation coefficient of $R^2 = 0.97$. The corresponding limit of detection (LOD) for *n*-pentane was calculated to be 758 ppm (Equation S2–4), which is below the immediately dangerous to life or health (IDLH) concentration of 1500 ppm. Similarly, for chloroform (Fig. 4f), a linear response was observed from 520 to 5200 ppm with an excellent fit ($R^2 = 0.99$), and the LOD was determined to be 259 ppm, also lower than the IDLH threshold of 500 ppm.

$$S_b = \sqrt{\frac{\sum_{i=1}^{n}\left(x_i - \bar{x}\right)}{n-1}} \quad \text{(S2)}$$

$$S = \frac{\Delta I}{\Delta c} \quad \text{(S3)}$$

$$DL = \frac{3S_b}{S} \quad \text{(S4)}$$

References

1 M. Xue, Q. Miao and Y. Fang, *Acta Physico-Chimica Sinica*, 2013, **29**, 2005-2012.

2 S. Kolemen, O. A. Bozdemir, Y. Cakmak, G. Barin, S. Erten-Ela, M. Marszalek, J.-H. Yum, S. M. Zakeeruddin, M. K. Nazeeruddin, M. Grätzel and A. E. U., *Chem. Sci.*, 2011, **2**, 949-954.

3 Y. Li, K. Liu, J. Liu, J. Peng, X. Feng, Y. Fang. *Langmuir*, 2006, **22**, 7016-7020.

4 J. Lakowicz, Principles of Fluorescence Spectroscopy, 3rd ed., chapter 6, pp208-210; Kluwer Academic/Plenum Publishers: New York, 1999.

5 M. Frisch, G. Trucks, H. Schlegel, G. Scuseria, M. Robb, J. Cheeseman, G. Scalmani, V. Barone, G. Petersson, H. Nakatsuji, X. Li, M. Caricato, A. Marenich, J. Bloino, B. Janesko, R. Gomperts,

B. Mennucci, H. Hratchian, J. Ortiz, A. Izmaylov, J. Sonnenberg, D. Williams-Young, F. Ding, F. Lipparini, F. Egidi, J. Goings, B. Peng, A. Petrone, T. Henderson, D. Ranasinghe, V. Zakrzewski, J. Gao, N. Rega, G. Zheng, W. Liang, M. Hada, M. Ehara, K. Toyota, R. Fukuda, J. Hasegawa, M.

Ishida, T. Nakajima, Y. Honda, O. Kitao, H. Nakai, T. Vreven, K. Throssell, J. Montgomery, Jr., J. Peralta, F. Ogliaro, M. Bearpark, J. Heyd, E. Brothers, K. Kudin, V. Staroverov, T. Keith, R. Kobayashi, J. Normand, K. Raghavachari, A. Rendell, J. Burant, S. Iyengar, J. Tomasi, M. Cossi, J. Millam, M. Klene, C. Adamo, R. Cammi, J. Ochterski, R. Martin, K. Morokuma, O. Farkas, J. Foresman and D. Fox, Gaussian 16, Revision A.03, Gaussian, Inc., Wallingford, CT, 2016.

6. L. Curtiss, M. McGrath, J.-P. Blaudeau, N. Davis, R. Binning, Jr. and L. Radom, *J. Chem. Phys.*, 1995, **103**, 6104–6113.
7. J. Tomasi, B. Mennucci and R. Cammi, *Chem. Rev.*, 2005, **105**, 2999–3094.
8. G. Scalmani, M. J. Frisch, B. Mennucci, J. Tomasi, R. Cammi and V. Barone, *J. Chem. Phys.*, 2006, **124**, 094107.